



Cite this: RSC Adv., 2019, 9, 31370

Received 3rd July 2019
 Accepted 23rd September 2019
 DOI: 10.1039/c9ra05034e
rsc.li/rsc-advances

1. Introduction

Huge amounts of pharmaceuticals are used every year by humans throughout the world.^{1,2} For example, 836 tons acetysalicylic acid, 622 tons paracetamol, 345 tons ibuprofen and 86 tons diclofenac were used in Germany in 2001.³ Diclofenac (DCF), a widely used non-steroidal anti-inflammatory drug, was frequently detected in groundwater, treated sewage and surface water in recent years.^{4,5} It could hardly be removed completely by the conventional wastewater treatment plants. Thus, the effluent of raw and treated sewage was considered to be its primarily pathway entering the environment.^{6,7} Oaks *et al.*⁸ reported that DCF could cause a high death rate among three species of vulture in India and Pakistan. The biological toxicity of DCF may also induce a risk to the other organisms or even human health. As a result, its risk should be paid urgent attention though its concentration in the natural environment is very low.

Advanced oxidation processes (AOPs) have received significant attention for the degradation of emerging contaminants in recent years.^{9–11} AOPs are characterized by the production of active radicals, such as hydroxyl radical (HO^\bullet), sulfate radical ($\text{SO}_4^{\cdot-}$) and carbonate radical ($\text{CO}_3^{\cdot-}$), which are very reactive and even can mineralize organic pollutants thoroughly. Hydroxyl radical-based AOPs ($E^\circ = 2.8$ V), including Fenton, photo-Fenton, UV/ H_2O_2 and $\text{O}_3/\text{H}_2\text{O}_2$, are widely investigated in last decades.^{11–13} Recently, considerable papers about the

degradation of DCF by hydroxyl radical-based AOPs were reported, such as UV/ H_2O_2 ,¹² photo-Fenton,¹⁴ UV/ TiO_2 ,¹⁵ etc. In addition, sulfate radical ($E^\circ = 2.5\text{--}3.1$ V) and carbonate radical ($E^\circ = 1.78$ V at pH 7) also drew public attention because of their selectivity and high oxidation capability.^{9,16,17} Particularly, sulfate radical (SR)-based AOPs have caused more attention, because $\text{SO}_4^{\cdot-}$ can be readily generated through transition metal, UV or heat activation of cheap oxidants (e.g., persulfate (PS) and peroxymonosulfate (PMS)) and these technologies have achieved success in the elimination of many emerging contaminants. Of which heat-activated persulfate (HAP) is a relatively green SR-AOPs which will not bring secondary pollution though it needs energy input. Therefore, HAP has been widely studied to degrade amounts of organic compounds such as duron,¹⁸ carbamazepine,¹⁹ *p*-nitrophenol,²⁰ benzoic acid,²¹ triclosan²² and so on. The degradation of DCF by HAP was also investigated by Chen *et al.*,²³ but its reaction mechanism in this system is still unclear until now. Besides, although the influence of several water matrix (e.g., Cl^- , HCO_3^- , and natural organic matter (NOM)) on DCF removal were explored in their study, the effect of the other constituents such as CO_3^{2-} , SO_4^{2-} , NO_3^- , Fe^{3+} , and Cu^{2+} were not investigated. Accordingly, the removal of DCF by HAP was systematically investigated in this study including degradation kinetics, influence factors and transformation mechanism.

The main objectives of this work were: (i) to investigate the effect of common water matrix including metal cations (e.g., Fe^{3+} and Cu^{2+}), inorganic anions (i.e., CO_3^{2-} , SO_4^{2-} and NO_3^-) and NOM on DCF degradation; (ii) to detect the transformation products of DCF for speculating its degradation mechanism by

Faculty of Geosciences and Environmental Engineering, Southwest Jiaotong University, Chengdu 611756, China. E-mail: liuyq@swjtu.edu.cn



HAP; and (iii) to identify the dominant reactive radical species and quantify their contribution to DCF removal in HAP system at different pH values through the radical scavenging experiments based on the fact that the radical species is dependent on the solution pH in SR-AOPs.

2. Materials and methods

2.1 Materials

Diclofenac sodium (99%) was obtained from Aladdin (China). Methanol, acetic acid, isopropanol and *tert*-butanol were all HPLC grade and purchased from Kelong (Chengdu, China). All the other reagents were AR grade and used without further purification. Milli-Q water (18 MΩ cm) was used for preparing all aqueous solutions.

2.2 Experimental setup

All experiments were carried out in a 1 L glass beaker containing 600 mL reaction solution. Before adding DCF and the other chemicals, the reactor was pre-heated in a thermostat water bath for about 30 min to reach to the desired temperature. Then, DCF standard solution was added into the reaction solution and its initial concentration was 1 μM. After that, the solution was stirred rapidly for several minutes by a mechanical agitator, ensuring a complete mixing of solution. Finally, appropriate volume of 6 mM persulfate was added into the solution, and the reaction began. At given time intervals, 1.5 mL reaction solution was sampled and fleetly quenched with 0.45 M Na₂S₂O₃. All the experiments were conducted in triplicate. The error bars in the figures represent the standard error of the mean.

2.3 Chemical analysis

The concentration of DCF was determined by a high performance liquid chromatograph (HPLC, Waters 2695, USA) equipped with a symmetry C18 column (5 μm, 4.6 × 150 mm) and a UV detector (Waters 2966, USA) at 276 nm. The mobile phase consisted of methanol and 1% acetic acid water solution (75/25, v/v) with a flow rate of 1.0 mL min⁻¹. The column temperature was 30 °C and the sample injection volume was 20 μL. pH was measured by a pH meter (INESA Scientific Instrument Co., Ltd, China). The transformation products of DCF were detected using an ultra performance liquid chromatograph coupled with a quadrupole-time of flight-mass spectrometry (UPLC-QTOF/MS, Waters Xevo G2-XS QT, USA). The chromatographic separation was performed on a C18 column (1.7 μm, 2.1 × 100 mm) with the sample injection volume of 10 μL. The mobile phase contained A (0.1% formic acid in water) and B (acetonitrile) at the flow rate of 0.3 mL min⁻¹. The gradient was 10% B in the initial 0.5 min, linearly increasing to 100% B for 6.5 min, and decreasing back to 10% B for 3 min. The mass spectrum (*m/z* 50–800) was analyzed in a positive ion mode by electrospray ionization (ESI) with the drying gas temperature of 400 °C and capillary voltage of 2.5 kV. Data were analyzed through Masslynx 4.1 software (Waters, USA).

3. Results and discussion

3.1 Degradation of DCF by HAP

Fig. 1 shows the degradation of DCF by heat alone, PS alone and HAP. DCF was hardly degraded after 60 min by heat alone and PS alone, while about 96% DCF was removed after 30 min with the addition of persulfate at 70 °C which was probably due to the role of the formed radicals from the activated PS by heat. The degradation of DCF in HAP system followed a pseudo-first-order kinetic model, and the observed degradation rate constant was thus calculated to be 0.103 min⁻¹ according to eqn (1).

$$-\frac{d[DCF]}{dt} = k_{obs}[DCF] \quad (1)$$

where k_{obs} is the pseudo-first-order rate constant of DCF by HAP, and [DCF] is the molar concentration of DCF at any time.

3.2 Effect of initial pH

The solution pH can affect the species and concentration of active radicals (*i.e.*, HO[·] and SO₄²⁻) in SR-AOPs, which may influence the degradation of organic contaminants.^{24,25} The effect of pH (3.0–11.0) on DCF degradation is shown in Fig. 2. The removal rate of DCF at pH 3 ($k_{obs} = 0.48 \text{ min}^{-1}$) was remarkably higher than those at the other pH values. At the strong acid condition, Caro's acid (H₂SO₅) might be formed, as shown in eqn (2), and its redox potential was reported to be 1.50 V.^{26,27} To clarify if DCF could be oxidized by the formed H₂SO₅, the removal of DCF in the presence of persulfate under the room temperature (25 °C) at pH 3 was investigated. As shown in Fig. 2, DCF could hardly be degraded in this reaction condition, indicating that it could not be removed by H₂SO₅ oxidation. Therefore, the fastest DCF degradation at pH 3 might be ascribed to the increase in the steady-state concentration of reactive radicals in this system, because the structure of Caro's acid was similar to that of peroxymonosulfate, leading to its possible activation by heat to produce HO[·] and SO₄²⁻, as presented in eqn (3).²⁸ To verify the above speculation, two different alcohols,

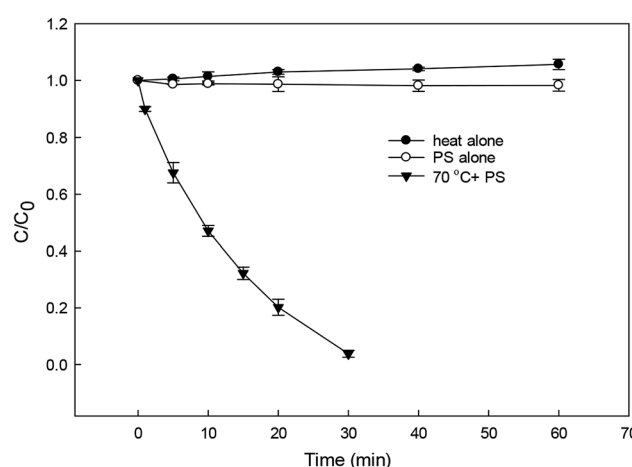


Fig. 1 Degradation of DCF by different reaction systems. Experimental conditions: [DCF]₀ = 1 μM, [PS]₀ = 50 μM, no buffer, $T = 25 \text{ }^{\circ}\text{C}$ for PS alone system, $T = 70 \text{ }^{\circ}\text{C}$ for heat alone and HAP systems.



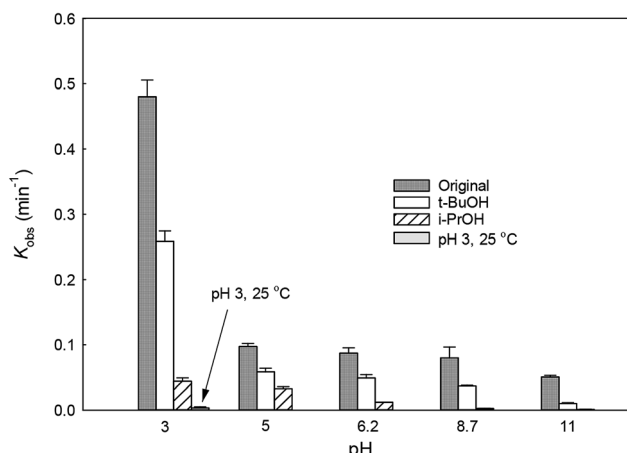


Fig. 2 Variation of k_{obs} as a function of initial pH for DCF degradation. Experimental conditions: $[\text{DCF}]_0 = 1 \mu\text{M}$, $[\text{PS}]_0 = 50 \mu\text{M}$, $[\text{t-BuOH}]_0 = [\text{i-PrOH}]_0 = 5 \text{ mM}$, $T = 70^\circ\text{C}$ ($T = 25^\circ\text{C}$ for verifying group at pH 3), 5 mM phosphate buffer.

i.e., *tert*-butanol (*t*-BuOH, $k_{\text{SO}_4^{\cdot-}/\text{t-BuOH}} = (4 - 9.1) \times 10^5 \text{ M}^{-1} \text{ s}^{-1}$, $k_{\text{HO}^{\cdot}/\text{t-BuOH}} = (4.2 - 7.6) \times 10^8 \text{ M}^{-1} \text{ s}^{-1}$) and isopropanol (i-PrOH, $k_{\text{SO}_4^{\cdot-}/\text{i-PrOH}} = (3.2 - 9.1) \times 10^7 \text{ M}^{-1} \text{ s}^{-1}$, $k_{\text{HO}^{\cdot}/\text{i-PrOH}} = (1.6 - 2.3) \times 10^9 \text{ M}^{-1} \text{ s}^{-1}$), were added into this system, respectively.²⁹⁻³¹ As shown in Fig. 2, due to the scavenging of *t*-BuOH for HO^{\cdot} , the degradation of DCF at pH 3 was inhibited significantly with its addition. While the inhibition effect was more obvious in the presence of i-PrOH, because it could also react with $\text{SO}_4^{\cdot-}$ except quenching HO^{\cdot} . This radical scavenging experiment indicated that $\text{SO}_4^{\cdot-}$ and HO^{\cdot} were both present and responsible for DCF removal by HAP at pH 3 and their contribution to DCF degradation were 54% and 46%, respectively.

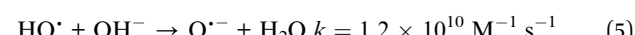


With the increase of initial pH from 5 to 11, the concentration of OH^{\cdot} in the solution increased gradually. It could react with $\text{SO}_4^{\cdot-}$, as presented in eqn (4), lowering the contribution of this radical to DCF removal,³² which was also confirmed by the radical scavenging experiments where the contribution of $\text{SO}_4^{\cdot-}$ to DCF degradation were 60.4%, 56.4%, 46.2% and 20.1% at pH 5, 6.2, 8.7 and 11, respectively, as described in Fig. 2 and Table 1. Although HO^{\cdot} could be formed from the above reaction, it could also be scavenged by OH^{\cdot} and $\text{SO}_4^{\cdot-}$, as shown in eqn (5)

Table 1 Contribution of reactive radical species to DCF degradation in HAP system at different pH values

pH	k_{obs} (min^{-1})	$\text{SO}_4^{\cdot-}$ (%)	HO^{\cdot} (%)
3	0.480	54	46
5	0.097	60.4	39.6
6.2	0.087	56.4	43.6
8.7	0.080	46.2	53.8
11	0.050	20.1	79.9

and (6).³² Hence, the degradation rate of DCF declined from 0.097 to 0.050 min^{-1} when the initial pH changed from 5 to 11. According to these results, we could conclude that except pH 3, $\text{SO}_4^{\cdot-}$ was the dominant radical species at pH < 7; while HO^{\cdot} became the main radical at high pH condition in HAP system. Similar conclusion was also obtained by Tan *et al.*³³ Overall, HAP was considered to be an efficient treatment technology for the degradation of DCF because of its effectiveness in a broad range of pH, especially at pH ≤ 3 .



3.3 Effect of reaction temperature

The effect of temperature on DCF degradation in a range of 30–80 °C is shown in Fig. 3. When the reaction temperature was 30 °C and 40 °C, DCF could hardly be degraded. As the temperature increased, the persulfate could gradually be activated readily to produce $\text{SO}_4^{\cdot-}$ leading to the enhancement of its steady-state concentration. Meanwhile, the collision probability between DCF and the reactive radicals might be improved with the increasing temperature based on the thermodynamics principle.³⁴ Therefore, the k_{obs} increased from 0.007 to 0.207 min^{-1} when the temperature changed from 50 to 80 °C. Most of the published papers on HAP system all found that the degradation of organic contaminant was faster in the higher temperature.^{33,35,36}

The plot of $\ln k_{\text{obs}}$ vs. $1/T$ (the insert in Fig. 3) showed an excellent fit with the Arrhenius type model (eqn (7)). The activation energy of DCF degradation by HAP was thus calculated to be 101.4 kJ mol⁻¹ in this study. However, Chen *et al.*²³ reported that the activation energy of this reaction was 157.63 kJ mol⁻¹,

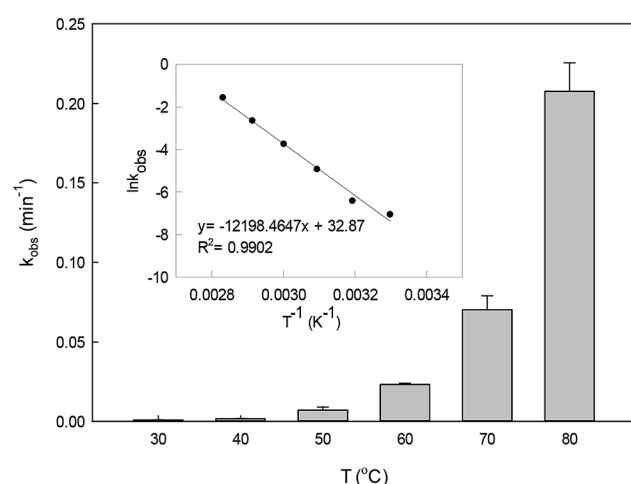


Fig. 3 Effect of temperature on k_{obs} in HAP system. The inset is the Arrhenius plot for DCF degradation. Experimental conditions: $[\text{DCF}]_0 = 1 \mu\text{M}$, $[\text{PS}]_0 = 50 \mu\text{M}$, 5 mM phosphate buffer at pH 6.2.



which was higher than that obtained by this study. This disagreement might be due to the difference of the reaction conditions between their study ($\text{pH} = 7$) and ours ($\text{pH} = 6.2$).

$$\ln k_{\text{obs}} = \ln A - \frac{E_A}{RT} \quad (7)$$

where A is the pre-exponential factor, E_A is the apparent activation energy of the reaction, R is the universal gas constant ($8.314 \text{ J mol}^{-1} \text{ K}^{-1}$), and T is the absolute temperature.

3.4 Effect of initial PS dosage

The dosage of PS is an important parameter in SR-AOPs, which can influence the degradation of target pollutants. Many researches have found that within the definite range of PS concentration, the degradation of organic contaminants enhanced with the increase in its dosage. Similar result was also obtained in our study on DCF removal by HAP, as shown in Fig. 4. The degradation rate of DCF enhanced from 0.003 min^{-1} to 0.087 min^{-1} as the concentration of PS increased from 1 to 50 μM . The increase of PS dosage could produce more active radicals in HAP system, leading to the improvement on DCF degradation.

3.5 Effect of water matrix

3.5.1 Effect of metal cations. The effect of Fe^{3+} and Cu^{2+} (0–10 μM) on DCF degradation in HAP system at 70°C was investigated. As shown in Fig. 5a, Fe^{3+} was found to be no obvious impact on the degradation of DCF. Anipsitakis *et al.*³⁷ also reported that the persulfate could not be activated by $\text{Fe}^{(\text{III})}$. However, the addition of Cu^{2+} could significantly improve DCF degradation (Fig. 5b), which was in agreement with the results reported by Deng *et al.*¹⁹ and Zhang *et al.*²⁰ The improvement effect enhanced gradually with the increase of Cu^{2+} concentration. Possible explanations for this result include: (1) PS could be activated by Cu^{2+} to produce $\text{SO}_4^{\cdot-}$, as shown in eqn (8), increasing the steady-state concentration of $\text{SO}_4^{\cdot-}$ in HAP system;³⁸ (2) the formed Cu^{3+} possessed a high oxidation

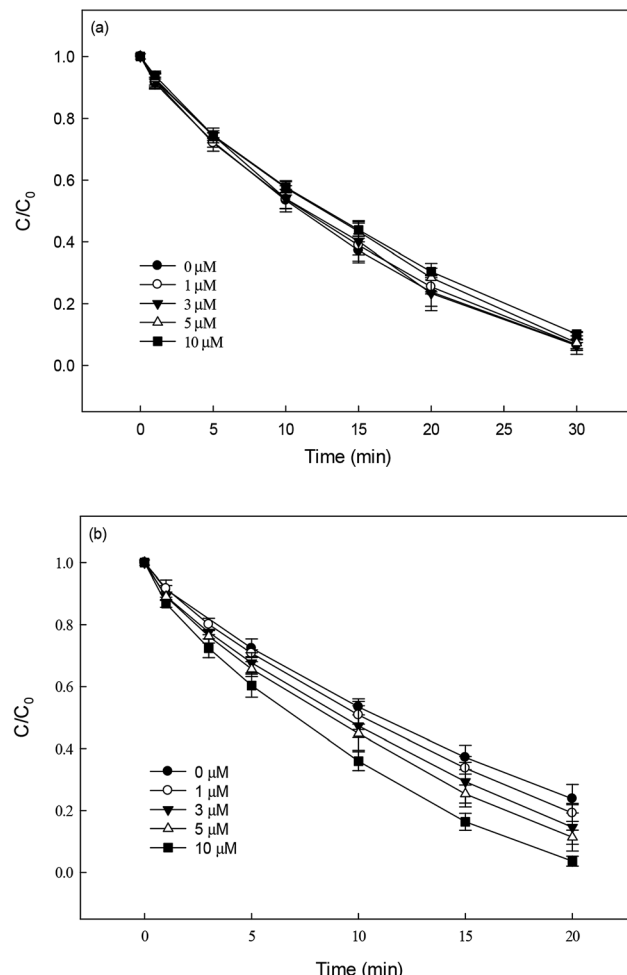


Fig. 5 Effect of Fe^{3+} (a) and Cu^{2+} (b) on DCF degradation in HAP system. Experimental conditions: $[\text{DCF}]_0 = 1 \mu\text{M}$, $[\text{PS}]_0 = 50 \mu\text{M}$, 5 mM phosphate buffer at pH 6.2.

capability and might be responsible for DCF degradation at a certain extent.¹⁹

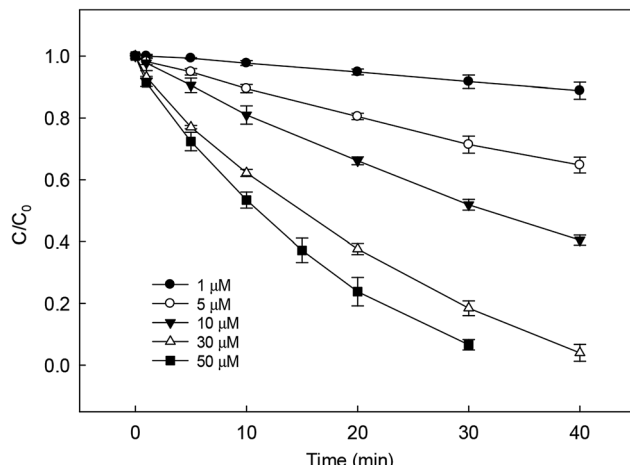
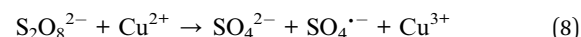


Fig. 4 Effect of initial PS dosage on DCF removal by HAP. Experimental conditions: $[\text{DCF}]_0 = 1 \mu\text{M}$, 5 mM phosphate buffer at pH 6.2.

3.5.2 Effect of inorganic anions. Nitrate (NO_3^-), sulfate (SO_4^{2-}) and carbonate (CO_3^{2-}) are common anions in natural water and may influence the degradation of target contaminant by SR-AOPs. Hence, their effect on DCF removal in HAP system was investigated, respectively. As shown in Fig. 6a and b, the degradation of DCF could hardly be influenced in the presence of various concentrations of NO_3^- and SO_4^{2-} , because they can scarcely react with $\text{SO}_4^{\cdot-}$.¹⁹ CO_3^{2-} is known to be an excellent scavenger for HO^{\cdot} and $\text{SO}_4^{\cdot-}$, which may inhibit the removal of organic pollutants in AOPs.^{18,39} However, an enhancement effect on DCF degradation by HAP was observed in our study, as presented in Fig. 6c. The presence of CO_3^{2-} could change the pH of the solution, and reached 10.3, 10.6 and 10.8 when the concentration of carbonate was 1, 3 and 5 mM, respectively. To avoid the influence of pH on DCF removal, the degradation of



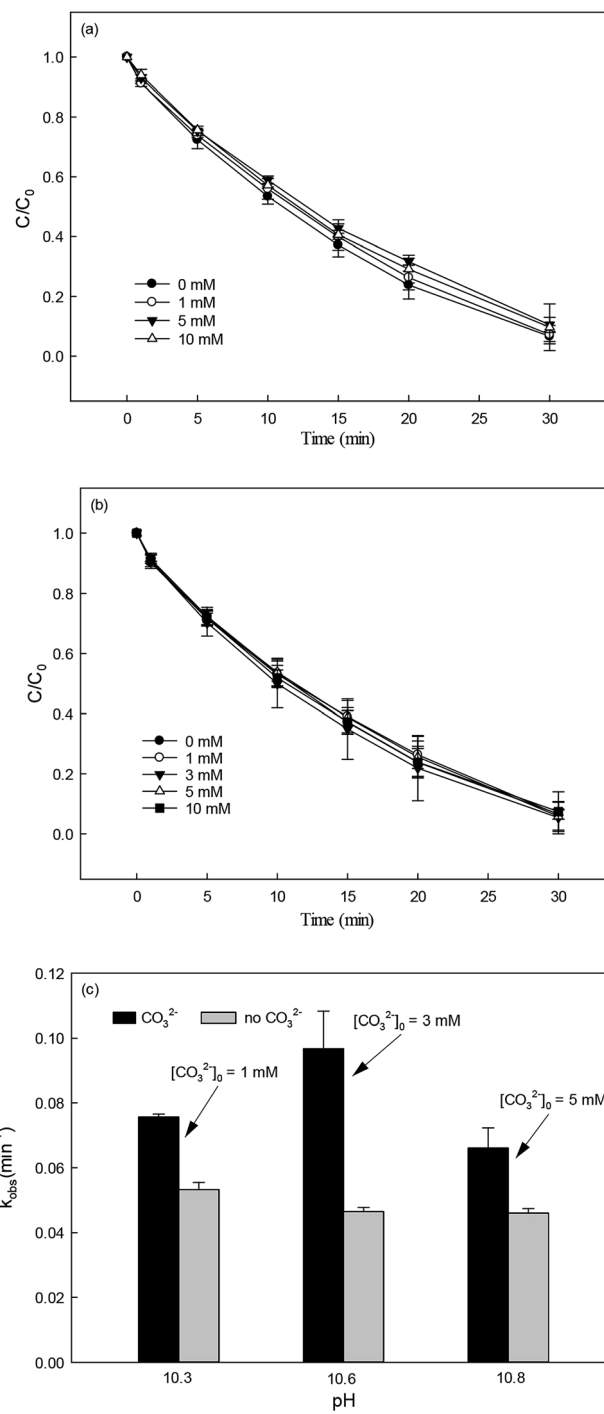
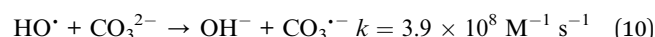
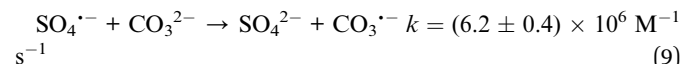


Fig. 6 Effect of NO_3^- (a), SO_4^{2-} (b) and CO_3^{2-} (c) on DCF degradation in HAP system. Experimental conditions: $[\text{DCF}]_0 = 1 \mu\text{M}$, $[\text{PSL}]_0 = 50 \mu\text{M}$, 5 mM phosphate buffer at pH = 6.2 for NO_3^- and SO_4^{2-} groups, no buffer for CO_3^{2-} group.

DCF by HAP at these pH values was conducted as a control system. Compared with the respective control system, the removal of DCF in the presence of CO_3^{2-} was obviously improved, which was probably attributed to the role of carbonate radical ($\text{CO}_3^{\cdot-}$) formed through the reactions of CO_3^{2-} with $\text{SO}_4^{\cdot-}$ and HO^{\cdot} , as presented in eqn (9) and (10).^{40,41}

Although the second-order rate constant of DCF with $\text{CO}_3^{\cdot-}$ ($k_{\text{CO}_3^{\cdot-}/\text{DCF}} = (2.7 \pm 0.7) \times 10^7 \text{ M}^{-1} \text{ s}^{-1}$)⁴² was lower than those with $\text{SO}_4^{\cdot-}$ ($k_{\text{SO}_4^{\cdot-}/\text{DCF}} = (9.2 \pm 0.6) \times 10^9 \text{ M}^{-1} \text{ s}^{-1}$)⁴³ and HO^{\cdot} ($k_{\text{HO}^{\cdot}/\text{DCF}} = (7.5 \pm 1.5) \times 10^9 \text{ M}^{-1} \text{ s}^{-1}$),¹¹ its steady-state concentration might be higher in the reaction system due to its selectivity,⁴⁴ resulting in a positive effect of CO_3^{2-} on DCF degradation. Similar finding was also reported by Huang *et al.*⁴² in DCF degradation by UV/ NO_3^- in the presence of HCO_3^- .



3.5.3 Effect of NOM. Natural organic matter is a common constituent in natural water. It can react with $\text{SO}_4^{\cdot-}$ and HO^{\cdot} due to its electron-rich moieties, resulting in an inhibition effect on the removal of target contaminant.^{25,45,46} In this study, humic acid (HA) and fulvic acid (FA) were chosen to represent NOM for investigating their effect on DCF degradation in HAP system. As shown in Fig. 7a and b, the presence of HA and FA

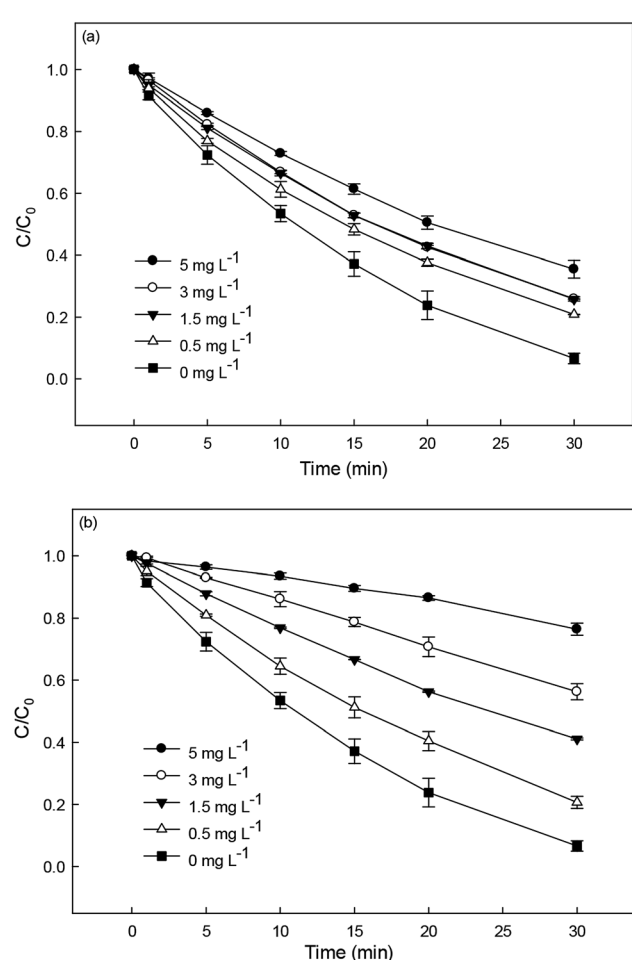


Fig. 7 Effect of HA (a) and FA (b) on DCF degradation in HAP system. Experimental conditions: $[\text{DCF}]_0 = 1 \mu\text{M}$, $[\text{PSL}]_0 = 50 \mu\text{M}$, 5 mM phosphate buffer at pH = 6.2.

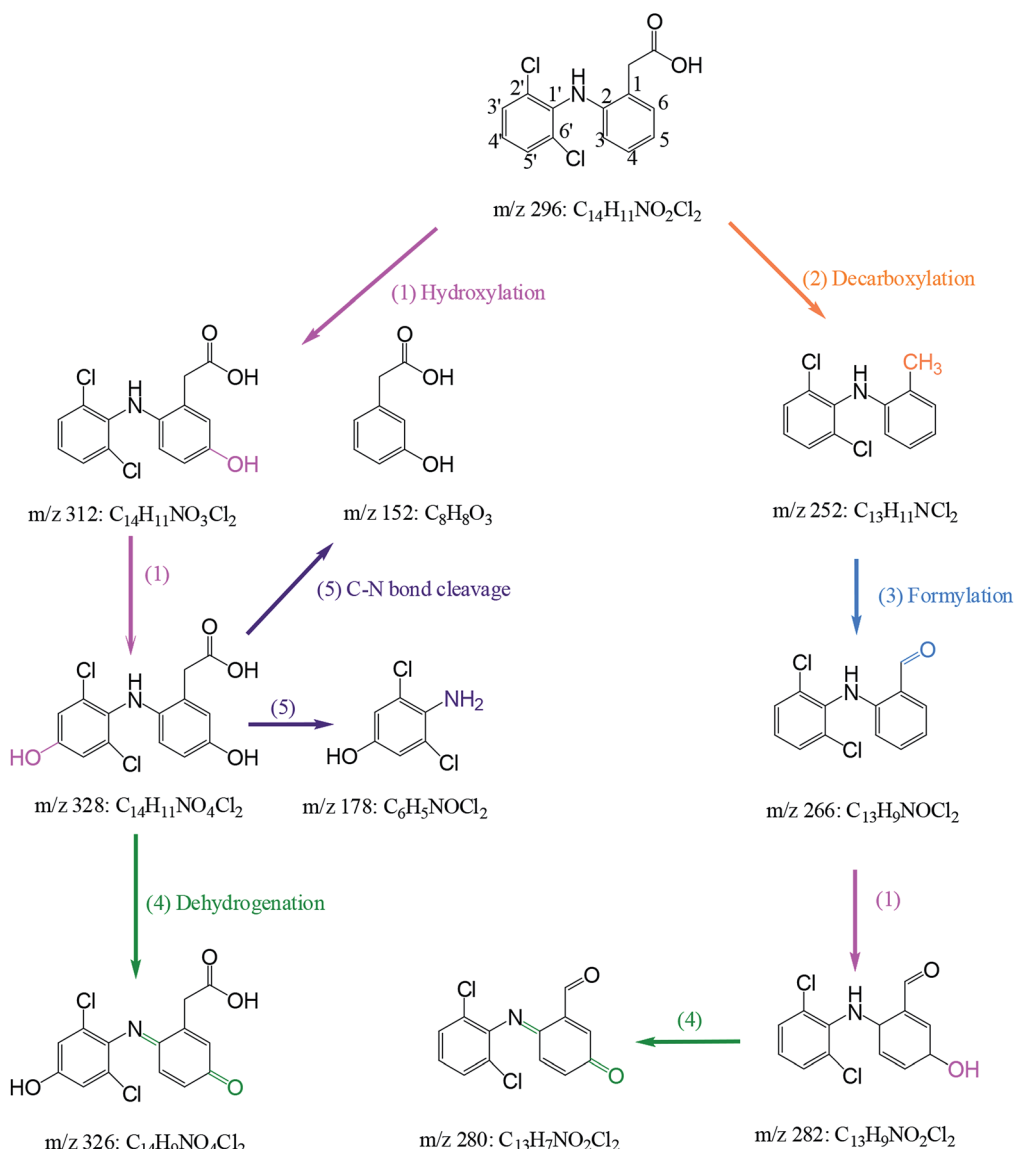
could both inhibit DCF degradation and the inhibition effect was more obvious with the increase of their concentrations. This was probably due to the competition of NOM with DCF for the reactive radicals. Compared with HA, the addition of FA showed a stronger inhibition on the degradation of DCF. However, it needs further investigation, because there is very limited available information on the reactivity of NOM toward $\text{SO}_4^{\cdot-}$.

3.6 Degradation mechanism of DCF by HAP

Nine transformation products (TPs) were detected during the degradation of DCF by HAP in this study. Based on these identified TPs, the potential DCF degradation mechanism was proposed, exhibiting five different transformation pathways including hydroxylation, decarboxylation, formylation, dehydrogenation and C–N bond cleavage, as depicted in Scheme 1.

(i) Hydroxylation (pathway (1) in Scheme 1) was an important pathway where DCF could be hydroxylated by the reactive radicals in HAP system. It is believed that $\text{SO}_4^{\cdot-}$ and HO^{\cdot} have the similar reaction mechanisms, including hydrogen abstraction, hydroxyl addition and electron transfer.^{32,47} In terms of DCF structure, aromatic ring might be a target site which was easily attacked by $\text{SO}_4^{\cdot-}$ due to its electron-rich nature. Therefore, monohydroxylation product 5-hydroxy-DCF (*m/z* 312) and dihydroxylation product 5,4'-hydroxy-DCF (*m/z* 328) were produced.

(ii) Decarboxylation (pathway (2) in Scheme 1) meant an elimination of $-\text{COOH}$ group from DCF structure. Phenylacetic acid structure on DCF might be attacked by $\text{SO}_4^{\cdot-}$ resulting in the transfer of an electron from aromatic ring to sulfate radical, and subsequently a $-\text{COOH}$ group could be removed from this structure *via* intramolecular electron transfer producing



Scheme 1 Proposed degradation mechanism of DCF by HAP: (1) hydroxylation, (2) decarboxylation, (3) formylation (4) dehydrogenation and (5) C–N bond cleavage. Experiment conditions: $[DCF]_0 = 1 \mu\text{M}$, $[PS]_0 = 50 \mu\text{M}$, no buffer.

a decarboxylation product m/z 252 (2-(2',6'-dichlorphenylamino)methylbenzene).⁴⁸ This product was also detected by Zhao *et al.*⁴⁹ and Liu *et al.*⁵⁰ in DCF degradation using ferrate(vi) and photoelectrocatalytic system, respectively.

(iii) Formylation (pathway (3) in Scheme 1) might result from the oxidation of the methyl group in the product m/z 252 leading to the formation of the product m/z 266 (2-(2',6'-dichlorophenylamino)benzaldehyde). The product m/z 282 might be further generated from the formed m/z 266 by hydroxylation.

(iv) Dehydrogenation (pathway (4) in Scheme 1) engaged in the oxidation of the -OH group at C5 and the -NH₂ group at C2 in the formed hydroxylation products. Zhou *et al.*⁵¹ reported that -OH and -NH₂ groups in the aromatic ring are two electron-donating groups, which increased the electron density in the *ortho*- and *para*-positions of aromatic ring and therefore attracted the attacks of SO₄²⁻ and HO[·]. As a result, two quinone imine products m/z 326 and 280 were generated from the products m/z 328 and 282 through dehydrogenation, respectively.

(v) C-N bond cleavage (pathway (5) in Scheme 1) occurred between two aromatic rings of the product m/z 328 by the attack of reactive radicals producing two products m/z 178 and 152. Similar transformation pathway was also reported by Chong *et al.*⁵² in the degradation of DCF using FeCeOx catalyzed H₂O₂.

4. Conclusions

This study systematically investigated the degradation of DCF under different experimental conditions by HAP. Compared to heat alone and PS alone systems, the degradation of DCF was significantly enhanced in HAP system at 70 °C and about 96% DCF was removed after 30 min. Its degradation in HAP system fitted with a pseudo-first-order kinetic model. The degradation rate of DCF decreased gradually with increasing pH and the highest k_{obs} was obtained at pH 3 probably due to the formation of Caro's acid. The radical scavenging experiments suggested that except pH 3, SO₄²⁻ was the dominant radical species at pH < 7; while HO[·] was mainly responsible for DCF degradation at high pH condition in HAP system. With the increase in the reaction temperature, the removal of DCF was improved, and the activation energy of this reaction was calculated to be 101.4 kJ mol⁻¹. Increasing initial dosage of PS could enhance the elimination of DCF. Presence of Cu²⁺ and CO₃²⁻ could improve DCF degradation, while an inhibition effect was observed in the presence of NOM. The other water constituents such as Fe³⁺, SO₄²⁻ and NO₃⁻ could hardly influence DCF removal. Nine degradation products of DCF were detected and identified using UPLC-QTOF/MS. Hence, the probable DCF transformation mechanism was proposed showing five different reaction pathways, including hydroxylation, decarboxylation, formylation, dehydrogenation and C-N bond cleavage.

Conflicts of interest

The authors declare no conflict of interest.

Acknowledgements

This work was supported by Sichuan Science and Technology Programs (No. 2017SZ0175 and No. 2018SZDZX0026). Yiqing Liu is also thankful to the financial support from the Fundamental Research Funds for the Central Universities (No. 2682018CX32).

References

- 1 A. Jelic, M. Gros, A. Ginebreda, R. Cespedes-Sánchez, F. Ventura, M. Petrovic and D. Barcelo, *Water Res.*, 2011, **45**, 1165–1176.
- 2 M. Carballa, F. Omil, J. M. Lema, M. Llompart, C. García-Jares, I. Rodríguez, M. Gómez and T. Ternes, *Water Res.*, 2004, **38**, 2918–2926.
- 3 K. Fent, A. A. Weston and D. Caminada, *Aquat. Toxicol.*, 2006, **76**, 122–159.
- 4 N. M. Vieno, H. Harkki, T. Tuhkanen and L. Kronberg, *Environ. Sci. Technol.*, 2007, **41**, 5077–5084.
- 5 Y. Zhang, S. U. Geißen and C. Gal, *Chemosphere*, 2008, **73**, 1151–1161.
- 6 S. K. Khetan and T. J. Collins, *Chem. Rev.*, 2007, **107**, 2319–2364.
- 7 I. S. Ruhoya and C. G. Daughton, *Environ. Int.*, 2008, **34**, 1157–1169.
- 8 J. L. Oaks, M. Gilbert, M. Z. Virani, R. T. Watson, C. U. Meteyer, B. A. Rideout, H. L. Shivaprasad, S. Ahmed, M. J. I. Chaudhry, M. Arshad, S. Mahmood, A. Ali and A. A. Khan, *Nature*, 2004, **427**, 630–633.
- 9 J. Wang and S. Z. Wang, *Chem. Eng. J.*, 2018, **334**, 1502–1517.
- 10 Y. Q. Liu, X. X. He, Y. S. Fu and D. D. Dionysiou, *Chem. Eng. J.*, 2016, **284**, 1317–1327.
- 11 M. M. Huber, S. Canonica, G. Y. Park and U. von Gunten, *Environ. Sci. Technol.*, 2003, **37**, 1016–1024.
- 12 D. Vogna, R. Marotta, A. Napolitano, R. Andreozzi and M. d'Ischia, *Water Res.*, 2004, **38**, 414–422.
- 13 M. Ravina, L. Campanella and J. Kiwi, *Water Res.*, 2002, **36**, 3553–3560.
- 14 L. A. Pérez-Estrada, S. Malato, W. Gernjak, A. Agüera, E. M. Thurman, I. Ferrer and A. R. Fernández-Alba, *Environ. Sci. Technol.*, 2005, **39**, 8300–8306.
- 15 A. Achilleos, E. Hapeshi, N. P. Xekoukoulotakis, D. Mantzavinos and D. Fatta-Kassinos, *Chem. Eng. J.*, 2010, **161**, 53–59.
- 16 P. Mazellier, C. Busset, A. Delmont and J. De Laat, *Water Res.*, 2007, **41**, 4585–4594.
- 17 F. Ghanbari and M. Moradi, *Chem. Eng. J.*, 2017, **310**, 41–62.
- 18 C. Q. Tan, N. Y. Gao, Y. Deng, N. An and J. Deng, *Chem. Eng. J.*, 2012, **203**, 294–300.
- 19 J. Deng, Y. S. Shao, N. Y. Gao, Y. Deng, S. Q. Zhou and X. H. Hu, *Chem. Eng. J.*, 2013, **228**, 765–771.
- 20 M. Zhang, X. Q. Chen, H. Zhou, M. Murugananthan and Y. R. Zhang, *Chem. Eng. J.*, 2015, **264**, 39–47.
- 21 N. Zrinyi and A. L. T. Pham, *Water Res.*, 2017, **120**, 43–51.
- 22 H. P. Gao, J. B. Chen, Y. L. Zhang and X. F. Zhou, *Chem. Eng. J.*, 2016, **306**, 522–530.



23 J. B. Chen, Y. J. Qian, H. M. Liu and T. Y. Huang, *Environ. Sci. Pollut. Res.*, 2016, **23**, 3824–3833.

24 C. J. Liang, Z. S. Wang and C. J. Bruell, *Chemosphere*, 2007, **66**, 106–113.

25 Y. Fan, D. Y. Kong, J. H. Lu and Q. S. Zhou, *J. Hazard. Mater.*, 2015, **300**, 39–47.

26 M. Spiro, *Electrochim. Acta*, 1979, **24**, 313–314.

27 I. M. Kolthoff and I. K. Miller, *J. Am. Chem. Soc.*, 1951, **73**, 3055–3059.

28 S. Y. Yang, P. Wang, X. Yang, L. Shan, W. Y. Zhang, X. T. Shao and R. Niu, *J. Hazard. Mater.*, 2010, **179**, 552–558.

29 G. V. Buxton, C. L. Greenstock, W. P. Helman and A. B. Ross, *J. Phys. Chem. Ref. Data*, 1988, **17**, 513–886.

30 C. L. Clifton and R. E. Huie, *Int. J. Chem. Kinet.*, 1989, **21**, 677–687.

31 P. Neta, R. E. Huie and A. B. Ross, *J. Phys. Chem. Ref. Data*, 1988, **17**, 1027–1284.

32 Y. Q. Liu, X. X. He, Y. S. Fu and D. D. Dionysiou, *J. Hazard. Mater.*, 2016, **305**, 229–239.

33 C. Q. Tan, N. Y. Gao, Y. Deng, W. L. Rong, S. D. Zhou and N. X. Lu, *Sep. Purif. Technol.*, 2013, **109**, 122–128.

34 Y. F. Ji, C. X. Dong, D. Y. Kong, J. H. Lu and Q. S. Zhou, *Chem. Eng. J.*, 2015, **263**, 45–54.

35 A. Ghauch, A. M. Tuqan and N. Kibbi, *Chem. Eng. J.*, 2012, **197**, 483–492.

36 R. H. Waldemer, P. G. Tratnyek, R. L. Johnson and J. T. Nurmi, *Environ. Sci. Technol.*, 2007, **41**, 1010–1015.

37 G. P. Anipsitakis and D. D. Dionysiou, *Environ. Sci. Technol.*, 2004, **38**, 3705–3712.

38 C. S. Liu, K. Shih, C. X. Sun and F. Wang, *Sci. Total Environ.*, 2012, **416**, 507–512.

39 J. Deng, Y. S. Shao, N. Y. Gao, S. J. Xia, C. Q. Tan, S. Q. Zhou and X. H. Hu, *Chem. Eng. J.*, 2013, **222**, 150–158.

40 Y. Q. Liu, X. X. He, X. D. Duan, Y. S. Fu and D. D. Dionysiou, *Chem. Eng. J.*, 2015, **276**, 113–121.

41 Y. Q. Liu, X. X. He, X. D. Duan, Y. S. Fu, D. Fatta-Kassinos and D. D. Dionysiou, *Water Res.*, 2016, **95**, 195–204.

42 Y. Huang, M. B. Kong, D. Westerman, E. G. Xu, S. Coffin, K. H. Cochran, Y. Q. Liu, S. D. Richardson, D. Schlenk and D. D. Dionysiou, *Environ. Sci. Technol.*, 2018, **52**, 12697–12707.

43 M. M. Ahmed, S. Barbati, P. Doumenq and S. Chiron, *Chem. Eng. J.*, 2012, **197**, 440–447.

44 J. P. Huang and S. A. Mabury, *Environ. Toxicol. Chem.*, 2009, **19**, 2181–2188.

45 P. Westerhoff, S. P. Mezyk, W. J. Cooper and D. Minakata, *Environ. Sci. Technol.*, 2007, **41**, 4640–4646.

46 P. M. D. Gara, G. N. Bosio, M. C. Gonzalez and D. O. Martire, *Int. J. Chem. Kinet.*, 2008, **40**, 19–24.

47 X. X. He, A. A. de la Cruz, K. E. O’shea and D. D. Dionysiou, *Water Res.*, 2014, **63**, 168–178.

48 V. Madhavan, H. Levanon and P. Neta, *Radiat. Res.*, 1978, **76**, 15–22.

49 J. F. Zhao, Y. Q. Liu, Q. Wang, Y. S. Fu, X. H. Lu and X. F. Bai, *Sep. Purif. Technol.*, 2018, **192**, 412–418.

50 S. S. Liu, X. Zhao, H. B. Zeng, Y. B. Wang, M. Qiao and W. Guan, *Chem. Eng. J.*, 2017, **320**, 168–177.

51 Z. W. Zhou and J. Q. Jiang, *J. Pharm. Biomed. Anal.*, 2015, **106**, 37–45.

52 S. Chong, G. M. Zhang, N. Zhang, Y. Liu, T. Huang and H. Chang, *J. Hazard. Mater.*, 2017, **334**, 150–159.

